Environmental and Experimental Botany 87 (2013) 1–9

Contents lists available at SciVerse ScienceDirect

Environmental and Experimental Botany

journal homepage: www.elsevier.com/locate/envexpbot

Accumulation of zinc and cadmium and localization of zinc in *Picris divaricata* Vant.

C. Leigh Broadhurst[a,b,*], Gary R. Bauchan[c], Charles A. Murphy[c], Ye-Tao Tang[d], Christopher Pooley[c], Allen P. Davis[b], Rufus L. Chaney[a]

[a] Environmental Management and Byproducts Utilization Laboratory, U.S. Department of Agriculture Henry A. Wallace Agricultural Research Center, 10300 Baltimore Blvd., Bldg. 007, Beltsville, MD 20705, USA
[b] Department of Civil and Environmental Engineering, University of Maryland, College Park, MD, USA
[c] Electron and Confocal Microscopy Unit, USDA ARS, Beltsville, USA
[d] School of Environmental Science and Engineering, Sun Yat-Sen University, Guangzhou, China

ARTICLE INFO

Article history:
Received 28 February 2012
Received in revised form 3 August 2012
Accepted 10 August 2012

Keywords:
Hyperaccumulator
Zinc
Cadmium
Phytoremediation
Trichome
Picris

ABSTRACT

Picris divaricata Vant., a plant species native to subtropical China, was recently identified as the first Cd/Zn hyperaccumulator from Asteraceae. *P. divaricata* was grown from wild collected seed for 4 months in a series of pH adjusted test soils with added Zn levels 0–7000 mg kg^{-1} and Cd levels 0–150 mg kg^{-1}. Plants did not hyperaccumulate Zn (threshold >3000 $\mu g\ g^{-1}$) and weakly hyperaccumulated Cd with little or no dose–response.

P. divaricata has multicellular simple trichomes concentrated on the leaf margins and midrib. X-ray analysis showed that Zn was concentrated in larger trichomes and epidermal cells adjacent to the trichome but virtually absent in other leaf tissues. Within the trichomes, Zn was localized in ovate spots around the tips of individual cells. These tips and other locations in the trichome cell contained black electron dense material when examined with transmission electron microscopy, some of which was identified as SiO_2. Silicon and Mn were concentrated in the same areas as Zn. Si has been previously associated with alleviating Zn, Mn and Cd toxicity. Our results support this observation and further investigation is warranted.

Calcium and P were concentrated in the distal tips of trichomes, similar to patterns previously observed for calcicole plants grown in elevated Ca soils. Overall, nonsecretory trichomes from many plant families may have a common origin as tissues adapted to handle a variety of environmental metals.

© 2012 Elsevier B.V. All rights reserved.

1. Introduction

Large areas of cultivated land in China, Japan and Thailand have been contaminated with Pb, Zn and Cd to the extent that demonstrable effects on human health have been reported (Kobayashi, 1978; Cai et al., 1990, 1995, 1998; Chaney et al., 2004; Teeyakasem et al., 2007; Phaenark et al., 2009). China in particular already has thousands of hectares of rice paddies contaminated with Cd, with the acreage increasing yearly (Tang et al., 2009). The extent of contamination virtually prohibits either removal and disposal of soils or agricultural disuse. Phytoremediation is one of the only viable options to remove excess metals from soils and return them to safe, productive use. Consequently there is a need for plants native to tropical and subtropical Asia that are suitable candidates for phytoremediation (Tang et al., 2009; Phaenark et al., 2009; Li et al., 2010). Cadmium phytoremediation is of particular urgency due to the widespread extent of contamination in Asia coupled with a low threshold for toxicity, and the central role of subsistence rice farming in reported cases of human Cd disease (Kobayashi, 1978; Chaney et al., 2004).

Candidate plants for phytoremediation must hyperaccumulate Cd in natural and anthropogenically contaminated soils which in most cases also contain 100–300 times higher concentrations of Zn, and possibly high levels of other metals including Pb, Cu, Ag and Mn. In some cases phytostabilization or phytoremediation of high Zn soils may be an additional objective. *Picris divaricata* Vant., native to subtropical China, has been recently identified as the first Cd/Zn hyperaccumulator from Asteraceae (Tang et al., 2009; Ying et al., 2010). However further study is required to confirm this and establish whether this plant is potentially useful for Cd/Zn phytoremediation/stabilization.

* Corresponding author at: Environmental Management and Byproducts Utilization Laboratory, U.S. Department of Agriculture Henry A. Wallace Agricultural Research Center, 10300 Baltimore Blvd., Bldg. 007, Beltsville, MD 20705, USA. Tel.: +1 301 504 6550.
E-mail address: leigh.broadhurst@ars.usda.gov (C.L. Broadhurst).

0098-8472/$ – see front matter © 2012 Elsevier B.V. All rights reserved.
http://dx.doi.org/10.1016/j.envexpbot.2012.08.010

In contrast to Ni hyperaccumulators, very little is known about the localization of Zn or Cd in tissues of hyperaccumulators. Küpper et al. (2000) and Zhao et al. (2000) found that Zn and Cd were consistently concentrated in epidermal cell vacuoles and at the base of leaf trichomes in *Arabidopsis halleri* (L. O'Kane & Al-Shehbaz) but not distributed throughout the trichome. In *Thlapsi caerulescens* (J.&C. Presl.), which does not have trichomes, Zn and Cd are localized in large epidermal cell vacuoles (Küpper et al., 1999; Frey et al., 2000; Leitenmaier and Küpper, 2011), a location strikingly similar to the trichome base. In *A. halleri*, *T. caerulescens* and three other European Zn hyperaccumulators, Zn was co-localized with Si in cell wall invaginations and vacuoles in epidermal and mesophyll cells (Neumann and zur Nieden, 2001; Neumann and De Figueiredo, 2002). Trichomes on these plants were not investigated.

In this contribution we have examined the ability of *P. divaricata* to hyperaccumulate Zn and Cd from test soils, and the localization of Zn within the plant leaf. *P. divaricata* has multicellular simple trichomes concentrated on the leaf margin and midrib. These trichomes have a complex and intriguing physiology that ties together many previous apparently disparate observations in plants adapted to metalliferous environments.

2. Materials and methods

2.1. Horticulture

P. divaricata seed was collected from wild plants growing in the Jiayashan mining area of the Lanping lead–zinc mining district Lanping County, Yunnan Province, China. It is the largest Pb/Zn mine in China and the second largest in Asia. In Lanping county, the reserves of Pb and Zn are 15.48 million tons, hemimorphite, smithsonite, sphalerite, cerusite and galena—primarily carbonates and silicates as opposed to massive sulfides. The geographic coordinates of the sampling site are 26°24′13″N, 99°25′35″E, and the altitude is 2670 m. The site has annual average temperature of 10.7–11.3 °C, annual average humidity of 74% and precipitation of 980–1010 mm (Tang et al., 2009).

Research plants were grown from seed in our greenhouse at USDA Beltsville, MD. Initial greenhouse growth testing utilized a mix of Palmerton, PA soil and Promix® potting soil which we have developed for successful *T. caerulescens* culture. The Palmerton soil was collected from an undisturbed partially wooded area about 0.5 km from a historic Zn smelting facility (dry soil contains 65 mg kg^{-1} Cd and 6450 mg kg^{-1} Zn). Some plants grown in Palmerton soil/Promix (50/50 vol% equivalent to 90/10 wt.%, pH 6.2) exhibited symptoms of Zn phytotoxicity but no mortality so these results were utilized to select the experimental treatment levels. Growth testing also showed that *P. divaricata* was intolerant of transplant and waterlogged soils, therefore, seeds were sown directly into prepared and equilibrated 250 ml pots.

The 250 ml pots contained Promix® soil with an increasing series of $ZnSO_4{\cdot}7H_2O$ (0, 1000, 3500, 7000 mg Zn kg^{-1}). Each Zn level also contained 75 mg Cd kg^{-1} (as $3CdSO_4{\cdot}8H_2O$). The 3500 and 7000 Zn levels were also prepared without Cd. For these treatments, $CaCO_3$ was added to each treatment at amounts equimolar with $ZnSO_4 + CdSO_4$ to correct the acidity generated by the metal salt additions. This adjustment sets the initial pH within 0.2 U of the Promix control (typically pH 6.5) so that experimental soil pH values do not differ greatly from control. Final (harvest) pH for each treatment was in the range 6.5–6.9 (Table 1). There were four replicates per treatment. Seedlings were thinned to two per pot if necessary but generally only a single seedling thrived and developed. Four replicates were also prepared with 5000 mg Zn kg^{-1} and 150 mg Cd kg^{-1} (a) without $CaCO_3$ addition (pH 5.20) and (b) with approximately half the equimolar $CaCO_3$ adjustment (pH 5.77).

Table 1
Whole leaf metal analyses in dry weight mg kg^{-1}.

Soil treatment, Zn/Cd (ppm)	pH	Ca (mg kg^{-1})	Cd (mg kg^{-1})	Cu (mg kg^{-1})	Fe (mg kg^{-1})	K (mg kg^{-1})	Mn (mg kg^{-1})	Zn (mg kg^{-1})
0/0	6.51	10,800 ± 754	dl	2.95 ± 0.655	68.7 ± 18.5	50,400 ± 10,200	103 ± 19.5	23.1 ± 3.48
1000/75	6.90	28,300 ± 22,300	89.5 ± 18.0	0.54 ± 0.39	40.9 ± 20.2	43,300 ± 22,500	84.2 ± 12.5	587 ± 131
5000/75	6.69	24,900 ± 4290	110 ± 21.0	0.91 ± 1.6	43.8 ± 12.3	37,500 ± 5490	181 ± 45.6	1930 ± 734
7000/75*	6.52	26,800	122	2.2	41.5	64,500	276	1820
3500/00	6.82	19,400 ± 5560	0.44 ± 0.41	1.88 ± 2.04	53.9 ± 24.7	48,000 ± 11,800	175 ± 65.3	1366 ± 475
7000/00*	6.38	11,900	1.2	2.6	29.8	86,300	150	1390
5000/150#	5.77	15,700	71.3	8.2	50.4	34,400	98.3	1209
5000/150#	5.77	15,900	81.6	7.3	76.1	32,200	94.0	1476

Mean of four analyses except for 7000 level plants (*) where only a single plant survived to harvest, and 150/5000 plants (#), with two only. Soil pH at harvest, initial pH for Cd 0 and 75 levels adjusted to be ±0.2 units of Promix (6.5). dl, detection limit.

The experiments were conducted in a greenhouse under controlled temperature conditions and ambient humidity. The experiment was conducted during the summer months therefore supplemental lighting was unnecessary. Daytime temperature was 24 °C with cooling initiated at 27 °C. Nighttime temperature was 18 °C with cooling initiated at 21 °C. Cooling was operational every day of the experiment for at least 14 h. A greenhouse roof shade cloth was in place throughout the summer to reduce overheating. Plants were grown in freely drained plastic pots with saucers to prevent loss of leachate, and watered with deionized water. The plants received standard fertilization (100 mg kg^{-1} N, P_2O_5, K_2O) a month after germination and each 3 weeks thereafter using a soluble fertilizer.

2.2. Total metals analysis

P. divaricata has elongate leaves that grow radially from a central tap root, thus the plant has almost no stem tissue until they bolt and bloom (Fig. 1). After 4 months of growth, leaves from various locations around the rosette were harvested for metal analysis. Leaves were rinsed in mild detergent solution and deionized water to remove any adhering soil particles. Leaf samples for each treatment were dried for 24 h at 60 °C, weighed, and ashed in a 480 °C oven for 16 h. After cooling, the ash was digested with 2 ml concentrated HNO_3 and heated to dryness. The sample was then dissolved in 10 ml 3 N HCl, filtered through Whatman #40 filter paper and brought to volume in a 25 ml volumetric flask using 0.1 N HCl. For quality control, reagent blanks and an in-house sunflower standard were included. Ca, Cd, Cu, Fe, K, Mg, Mn, P and Zn were determined by inductively coupled plasma atomic emission spectrometry using 40 mg L^{-1} yttrium as an internal standard in all samples and standard solutions.

2.3. X-ray and scanning electron microanalysis

For microanalysis, three smaller leaves of *P. divaricata* were harvested after 2 or 4 months of growth and immediately freeze-fractured. The samples were frozen conductively in a styrofoam box by placing the leaves on the surface of a pre-cooled brass bar whose lower half was submerged in liquid nitrogen. Each leaf was carefully fractured to yield complement cross-sections. One half was placed in a precooled vial and transferred to a storage dewar. Within a few days these leaf pieces were freeze-dried at −80 °C for X-ray analysis.

The other half of the complement fractures remained fully hydrated and were placed in a vertically slotted copper block specimen holder. Flat leaves were also examined on 16 mm × 30 mm copper plates. Leaves were secured with a thin layer of Tissue Tek (OCT Compound, Ted Pella, Inc., Redding, CA), which acts as the cryo-adhesive upon freezing.

Low-temperature SEM observations were performed using an S-4700 field emission scanning electron microscope (Hitachi High Technologies America, Inc., Pleasanton, CA) equipped with a Quorum PP2000 (Quorum Technologies Ltd., East Sussex, UK) cryotransfer system. The leaf samples on the copper holders were transferred under vacuum to the cold stage in the pre-chamber of the cryotransfer system.

Removal of any surface contamination (condensed water vapor) took place in the cryotransfer system by etching the frozen specimens for 10–15 min at a temperature of −90 °C. Following etching, the temperature was lowered to −130 °C, and a magnetron sputter head equipped with a platinum target was used to coat the specimens with a very thin layer of platinum. The specimens were transferred to a pre-cooled (−130 °C) cryostage in the SEM for observation. An accelerating voltage of 5 kV was used to view the specimens. Images were obtained using a 4pi Analysis System integrated to the SEM. Images were sized and placed together to produce the figures.

X-ray fluorescence analysis utilized a S-3700 Variable Pressure SEM (Hitachi High Technologies America, Inc., Pleasanton, CA) with a Deben Coolstage Peltier Stage (Deben UK Ltd., Suffolk, UK) set at −25 °C and an Oxford Instruments INCA® Electron Diffraction System (EDS) (NanoAnalysis, Bucks, UK). Images of uncoated freeze-dried leaves were obtained at 2000×. Samples were analyzed with 15 kV accelerating voltage, 10 mm working distance, and a 35° takeoff angle. Each spot location was counted for 300 or 600 live seconds, depending on the application (e.g. the delicate trichome tips may not remain stable for multiple analyses of 600 ls, so 300 ls or less is required). Beam spot size was 1–5 μm depending on the application but always less than a cell diameter when targeting a specific cell/location.

Elemental mapping was conducted for 2–4 h using INCA® mapping software. Elemental mapping was done at a dwell time of 200 μs, time constant of 50 μs, and resolution of 512 × 400 pixels. Every location that was mapped was digitally photographed.

The INCA software was utilized to calculate elemental concentrations normalized to 100 wt.% on an H free basis. Clearly the quantitative analysis program is not designed for heterogeneous biological materials with highly variable surface structure, therefore, these results serve only as a semi-quantitative guide to the relative amounts of heavier elements of interest such as Zn, Si, Ca and K.

2.4. Transmission electron microanalysis

Leaf tissue was cut into 1 mm pieces and fixed by immersion in 3% glutaraldehyde/0.05 M NaCacodylate buffer (pH 7.0) for 2 h at room temperature. This was followed by washing in a NaCacodylate buffer by rinsing 6 times for 1 h. Samples were placed into a refrigerator at 4 °C overnight. Next, samples were post fixed in 2% NaCacodylate buffered osmium tetroxide for 2 h at room temperature, dehydrated in acetone series and infiltrated with Spurrs low-viscosity embedding resin and cured in a 65 °C oven. Silver/gold, 90 nm sections were cut on a Riechert/AO Ultracut microtome with a Diatome diamond knife and mounted on 200 mesh Ni grids. One set of samples was stained with 4% uranyl acetate and 3% lead citrate and the other remained unstained in order to identify any artifacts that might be induced by adding additional heavy metals to the leaves. The unstained samples also skipped the osmium tetroxide step. Grids were viewed in a Hitachi HT-7700 microscope at 80 kV.

3. Results

Control, 1000, and 3500 Zn level plants grew normally with no symptoms of phytotoxicity. Not all seedlings at the 5000 level lived but those that did had only a few or no leaves with interveinal chlorosis. All replicates at the 7000 level exhibited weak growth and chlorosis; only two plants survived long enough to achieve adequate mass for total metals analysis. All plants without $CaCO_3$ addition died soon after germination. Similar to the 7000 level plants, plants with 5000 Zn and 150 Cd pH adjusted to 5.77 exhibited weak growth and chlorosis and only two survived long enough for total metals analysis (Fig. 1).

Dry weight element concentrations are given in Table 1. Although the leaves consistently accumulated over 1000 μg g^{-1} Zn and 100 μg g^{-1} Cd, they did not achieve the currently accepted threshold concentration for Zn hyperaccumulation of 3000 μg g^{-1} (van der Ent et al., 2012). In addition, plants with the 5000 Zn/150 Cd treatment and reduced soil pH did not accumulate more Zn or Cd than the 5000/75 plants. Initial test plants grown in Palmerton

Fig. 1. *Picris divaricata* (a) healthy plant in 250 g pot after 4 months growth in 80 vol% Promix and 20 vol% Palmerton, PA soil. Red coloration is normal response to strong light. (b) Plants in 5000 mg kg^{-1} Zn soil showing phytotoxicity symptoms including weak growth; small, yellow, brittle leaves; interveinal chlorosis. (c) Plant in 7000 mg kg^{-1} Zn soil showing extreme interveinal chlorosis with eventual mortality.

soil/Promix grew more vigorously than the experimental plants, however the Zn (2590 mg kg^{-1}) and Cd (59 mg kg^{-1}) concentrations were similar (full element data not given).

P. divaricata has two types of trichomes, small and large. The large trichomes are more numerous and occur in greatest density on the leaf margins and midribs. They are multicellular and usually bifurcated at the tip (Fig. 2). These trichomes appear simple, not glandular-secreting, and range in height from approximately 0.3 to 0.8 mm. Overall, the trichomes are relatively enriched in Ca, especially on the stalk and tip. The distal bifurcated tip was consistently enriched in P (1–7 wt.%); it was the only tissue analyzed with P concentrations over 1% (Table 2, Figs. 3 and 4).

X-ray analysis showed that Zn is highly concentrated in the large trichomes but not enriched in other types of leaf tissue (Table 2). Epidermal tissue not associated with trichomes had very little Zn; and Zn was near or below detection limits in the mesophyll and not

Table 2
Representative semi-quantitative X-ray elemental analyses in weight percent. Each sample also contained about 0.4% S which did not vary among locations and samples. Each value represents mean of 4–6 independent spot analyses in a given location/sample.

Sample and location	C	N	O	Mg	Si	P	Cl	K	Ca	Mn	Zn
5000/75											
Trichome stalk spot band I[a]	27 ± 1	2.0 ± 0.3	17 ± 0.8	0.31 ± 0.01	1.4 ± 0.1	0.13 ± 0.01	3.3 ± 0.2	8.4 ± 0.4	16 ± 0.7	1.1 ± 0.3	20 ± 0.7
Trichome stalk spot band II	24 ± 0.8	6 ± 0.6	24 ± 0.4	0.36 ± 0.01	0.25 ± 0.01	0.21 ± 0.01	2.2 ± 0.03	19 ± 0.3	17 ± 0.3	0.55 ± 0.15	5.6 ± 0.6
Trichome base spot I	47 ± 0.4	2.6 ± 0.2	34 ± 1	0.47 ± 0.02	0.35 ± 0.03	0.21 ± 0.01	1.5 ± 0.2	3.1 ± 0.07	6.0 ± 0.7	0.29 ± 0.06	2.6 ± 0.09
Trichome base spot II	50 ± 0.9	nd	36 ± 1	0.74 ± 0.02	0.80 ± 0.07	0.40 ± 0.01	1.3 ± 0.04	5.6 ± 0.08	3.6 ± 0.2	nd	4.0 ± 0.3
Trichome, distal tip	36 ± 0.6	3.3 ± 0.3	33 ± 0.4	0.95 ± 0.03	nd	7.1 ± 1	0.65 ± 0.03	6.7 ± 0.4	11 ± 0.8	0.27 ± 0.1	1.1 ± 0.2
Trichome base, general[b]	45 ± 0.6	4.5 ± 0.3	32 ± 0.4	0.44 ± 0.01	0.21 ± 0.03	0.22 ± 0.01	3.8 ± 0.05	12 ± 0.3	2.0 ± 0.06	nd	0.35 ± 0.03
Trichome, general	50 ± 1	3.4 ± 0.2	40 ± 5	0.76 ± 0.03	nd	0.33 ± 0.02	0.65 ± 0.02	3.4 ± 0.2	3.4 ± 0.2	nd	0.14 ± 0.03
Lower epidermis, general	50 ± 1	4.1 ± 0.3	31 ± 2	0.99 ± 0.06	nd	0.63 ± 0.08	1.2 ± 0.09	7.1 ± 0.5	3.9 ± 0.4	nd	0.11 ± 0.03
Mesophyll, adj. u. epiderm.	49 ± 0.9	7.9 ± 0.3	31 ± 2	0.55 ± 0.05	nd	0.63 ± 0.06	1.0 ± 0.07	7.1 ± 0.6	2.4 ± 0.3	nd	0.23 ± 0.09
3500/00											
Trichome stalk spot band I	38 ± 0.1	3.3 ± 0.4	15 ± 0.1	nd	0.35 ± 0.01	0.25 ± 0.01	1.4 ± 0.02	17 ± 0.2	8.3 ± 0.1	0.30 ± 0.03	17 ± 0.2
Trichome stalk spot band II	45 ± 0.3	2.4 ± 0.6	36 ± 1.2	0.38 ± 0.01	2.6 ± 0.1	0.67 ± 0.05	1.1 ± 0.04	1.8 ± 0.12	5.6 ± 0.2	0.37 ± 0.09	3.8 ± 0.3
Trichome base spot I	48 ± 0.1	2.2 ± 0.4	29 ± 0.2	0.36 ± 0.02	1.4 ± 0.02	0.28 ± 0.01	0.74 ± 0.01	7.7 ± 0.08	5.2 ± 0.02	0.15 ± 0.03	4.7 ± 0.1
Trichome base spot II	53 ± 8	3.2 ± 0.6	20 ± 2	nd	0.43 ± 0.08	0.32 ± 0.1	0.85 ± 0.3	13 ± 5	6.1 ± 2	nd	2.7 ± 0.5
Trichome, distal tip I	37 ± 0.8	3.1 ± 0.2	42 ± 0.8	0.43 ± 0.02	nd	1.1 ± 0.04	0.54 ± 0.04	6.3 ± 0.7	8.7 ± 0.5	0.19 ± 0.05	0.37 ± 0.14
Trichome, distal tip II	26 ± 0.6	3.4 ± 0.1	43 ± 0.7	0.49 ± 0.03	nd	3.9 ± 0.2	1.3 ± 0.08	14 ± 0.8	7.5 ± 0.4	0.35 ± 0.06	0.25 ± 0.07
Upper epidermis, general	52 ± 2	5.5 ± 0.3	36 ± 2	0.26 ± 0.03	nd	0.29 ± 0.01	0.38 ± 0.03	5.1 ± 0.3	0.71 ± 0.03	nd	nd
Mesophyll, adj. epidermis	40 ± 1	6.5 ± 0.1	26 ± 0.4	0.24 ± 0.0	nd	0.95 ± 0.2	0.50 ± 0.03	23 ± 0.5	2.2 ± 0.02	nd	0.17 ± 0.04
Mesophyll, central	54 ± 0.2	5.7 ± 0.2	33 ± 0.5	0.29 ± 0.01	nd	0.31 ± 0.02	0.45 ± 0.01	5.7 ± 0.2	0.79 ± 0.05	nd	nd

nd, not detected.

[a] Location also contained 1.6 ± 0.2 wt.% Ni and 2.1 ± 0.3 wt.%Cu.

[b] Access to interior via cross section of trichome.

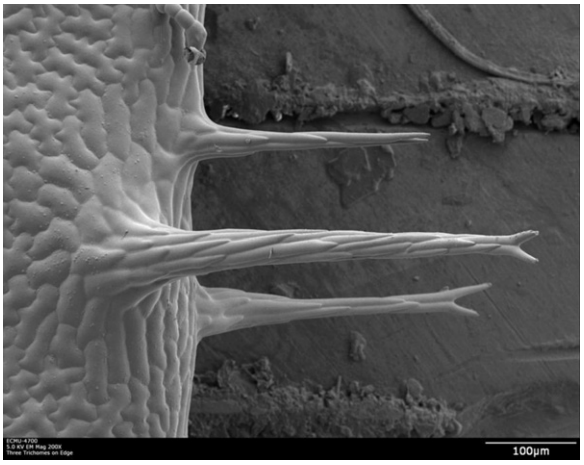

Fig. 2. Scanning electron photomicrograph of *P. divaricata* epidermal tissue with trichomes at leaf margin, frozen hydrated leaf 200×, 5.0 kV.

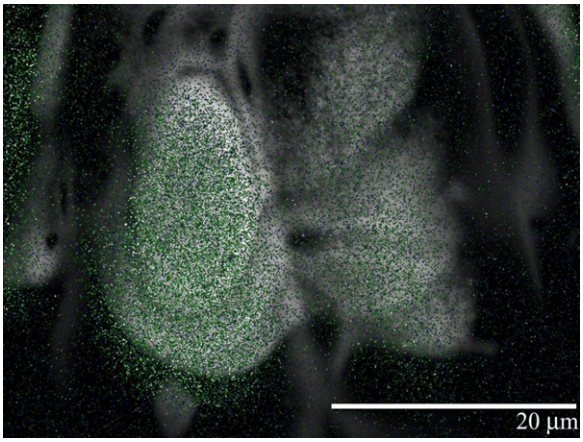

Fig. 4. X-ray map detail of trichome Zn "hot spot" halfway up stalk, 3500/0 sample. Zn counts in green, location spot analyses are listed in Table 2 with 17 wt.% Zn and 17 wt.% K. (For interpretation of the references to color in this figure legend, the reader is referred to the web version of this article.)

detected in vascular tissue. The mesophyll is undifferentiated with no clear distinction between spongy and palisade cells.

Within the trichomes Zn is strongly localized in ovate "spots" around the tips of individual trichome cells. These spots form a band or ring around the trichome, perpendicular to the long axis of growth, which is visible in the photomicrographs as a bright area, often with concentric rings (Fig. 4). Some of the largest (0.8 mm) trichomes have two or three bands, starting at the base and moving up the trichome as if the Zn-rich band moves up the trichome as growth occurs (Fig. 5). These bright bands are not visible in Fig. 1 due to the Pt coating. While some Zn was found in other areas of the trichome including the tip, the concentrations were much lower than in the spot bands. The material in the spot bands is not surface contamination or vascular excretion, and is unique to the larger trichomes.

X-ray spot analyses showed that dry weight Zn concentrations ranged from 3% to 20% when the beam was focused directly on the ovate spots. The lower range of concentrations (4–7%) was detected in spots near the base of the trichome, while the highest concentrations were found in spots or a broad band approximately midway up the trichome shaft. The high concentration "spot bands" are associated with the upper portions of several adjacent trichome cells. Cadmium concentrations were below detection limits for all

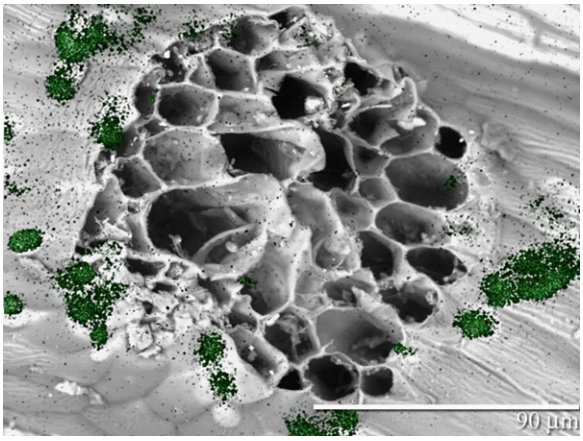

Fig. 5. Trichome guide photo of epidermal surface with trichome broken off at base, 5000/75 sample. Multicellular structure with relatively thin cell walls is evident. X-ray map of photo area is overlaid with Zn counts in green; higher Zn concentrations are found associated with light-colored spots in the trichome base.

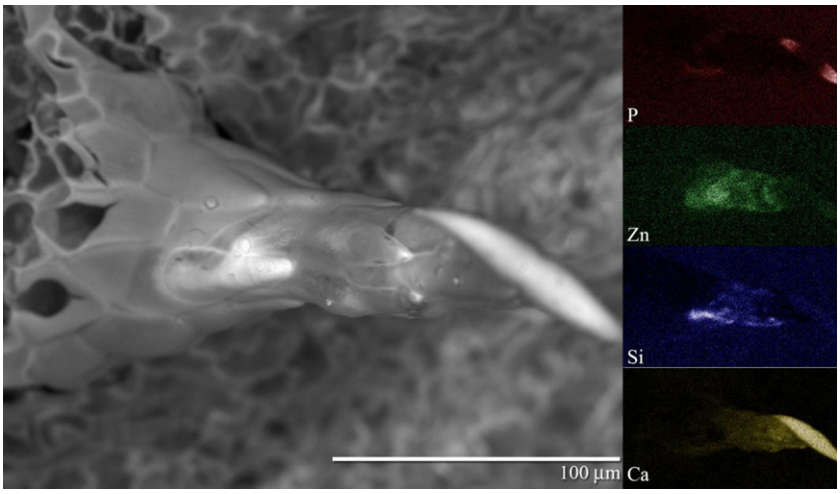

Fig. 3. *P. divaricata* trichome guide photo and X-ray maps of photo area, 15 kV, 5000/75 sample. Trichome tip is widely bifurcated in foreground to right of image. P is concentrated at trichome distal tip and Ca throughout trichome tip. Elevated Zn and Si concentrations are co-localized in the bright areas halfway up the trichome stalk. White areas within the colored areas represent the very highest concentrations.

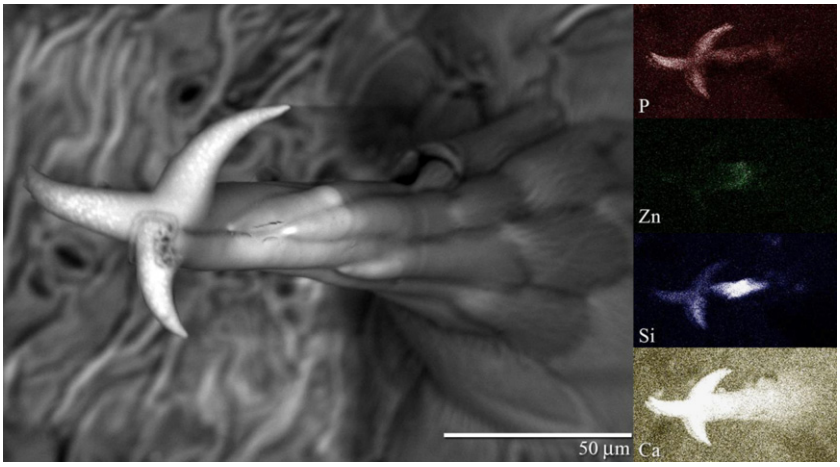

Fig. 6. Trichome guide photo and X-ray maps of photo area, 3500/0 sample. Trifurcated tip is relatively unusual. P is concentrated at trichome distal tip and Ca throughout trichome. The highest Si concentrations measured in any sample were in the bright areas halfway up the trichome stalk. Location spot analyses are listed in Table 2 with 2.6 wt.% Si. White areas within the colored areas represent the very highest concentrations.

spot analyses; a Cd signal just at detection limits was only observed when mapping the highest Zn areas for over 2 h.

Silicon was also concentrated in the same areas that were high in Zn, but not above background levels in any other leaf locations other than trichomes. On the 0.8 mm trichomes, we consistently detected Mn in the high Zn-spots that were mid-way up the shaft (Figs. 3 and 6). Since the weight percent calculation in Table 2 is semi-quantitative, Mn concentrations must generally be considered at or just over detection limits. However, Mn was not detected in any leaf tissue other than the spots. Further, Mn was not added to the experiment, yet the Mn concentrations in the spots were greater than the Zn concentrations in leaf mesophyll. Small amounts of Cu and Ni were detected in some trichomes and reached values over 1% in a spot band with 20% Zn (Table 2).

Transmission electron imaging revealed occasional dark, electron dense deposits associated mainly with epidermal tissue near or on trichomes, although some was seen in mesophyll adjacent to vascular tissue. These deposits appeared only in plants that had been treated with Zn, and were present in both stained and unstained samples, although staining enhanced contrast. Fig. 7 shows longitudinal cross sections of a trichome cell. Dark electron dense material appears in approximately the same locations where we observed the highest concentrations of Zn and Si. There was no indication that the electron dense material existed as a precipitate or particulate matter on the leaf surface. We were able to identify some of the electron dense material as SiO_2 (Fig. 8) but due to interference from the Ni grid we were unable to identify Zn.

4. Discussion

We did not confirm that *P. divaricata* is a Zn hyperaccumulator but it may be a reasonable Cd hyperaccumulator since Cd levels exceeded 100 $\mu g\,g^{-1}$ in the presence of significant Zn soil concentrations, and Cd bioaccumulation coefficients exceeded unity for most samples. The pH levels in our soils were in the same range or slightly lower than those in Tang et al. (2009), and within the range for typical productive soils. Overall, only 2 of 12 wild plant samples and 1 of 5 experimental treatments reported in Tang et al. (2009) exceeded the previously accepted 10,000 $\mu g\,g^{-1}$ standard for Zn hyperaccumulation, although 8 of 12 wild plants exceeded 3000 $\mu g\,g^{-1}$. The two locations where plants with over 10,000 $\mu g\,g^{-1}$ were collected had reported Zn soil concentrations of 11 and 13%—essentially a high-grade ore substrate. Further, the experimental mine waste soil had total Zn at 4.5% with pH 7.44. With these extremely high soil metal concentrations surface contamination of the leaves is probable (Faucon et al., 2007).

Even in the absence of such contamination, development of *P. divaricata* as a potential phytoremediation agent is in its early stages, and the strong variation in the wild collections may reflect different ecotypes, similar to the situation with *T. caerulescens*. There was also a large variability in the leaf Zn concentrations for plants at the various sampling locations (Tang et al., 2009) which mainly reflects varying soil concentrations, whereas a typical hyperaccumulator tends toward a plateau metal concentration that is not strongly dependent on the soil concentration.

We observed variability in plant growth from the wild seeds, and only two plants were able to survive at the 7000 ppm Zn soil level, or at a soil pH below 6.0. All plants in pH 5.2 soil died. Therefore *P. divaricata* may not be suitable for Cd/Zn phytoremediation in acidic soils; for example those associated with high-sulfide ores or tailings.

Another aspect to the variability is the potential for interaction with soil Mn. We previously identified a strong correlation between the localization of Ni and Mn in the trichomes of *Alyssum* Ni hyperaccumulators (Broadhurst et al., 2004, 2009, submitted for publication). The relationship was first identified in an experiment in which Mn was not added beyond normal potting soil levels, than in both soil and hydroponic experiments in which Mn was purposely increased. If a consistently performing Zn/Cd ecotype is identified and developed, experimentation with increasing Mn levels would be a logical next step due to the intriguing possibility that Mn localization in trichomes of normal, metal tolerant, and hyperaccumulator species may be relatively common and based upon a fundamental pathway. Additionally, soil Mn levels could influence uptake and accumulation of Zn and Cd in *P. divaricata*, thus become a contributing factor in the previously observed variability (Tang et al., 2009) in the Zn/Cd concentrations between locations.

While Cd was below X-ray detection limits in this study, the "spot band" area corresponds exactly to the location where Cd was observed in a recent X-ray study of *P. divaricata* grown hydroponically without excess Zn (Hu et al., 2012). Cadmium was also localized in trichomes in *Arabidopsis thaliana*, which is not a Zn/Cd hyperaccumulator but closely related to the hyperaccumulator *A. halleri*. In particular, Cd, P and Mn were localized in a band in the trichome trunk, and Cd, Cl, Mn and Si localized in the trichome tips (Isaure et al., 2006). However, Isaure et al. (2006) utilized 12-day-old seedlings grown in agar culture without excess Zn. Other short-term agar or hydroponic culture without excess Zn

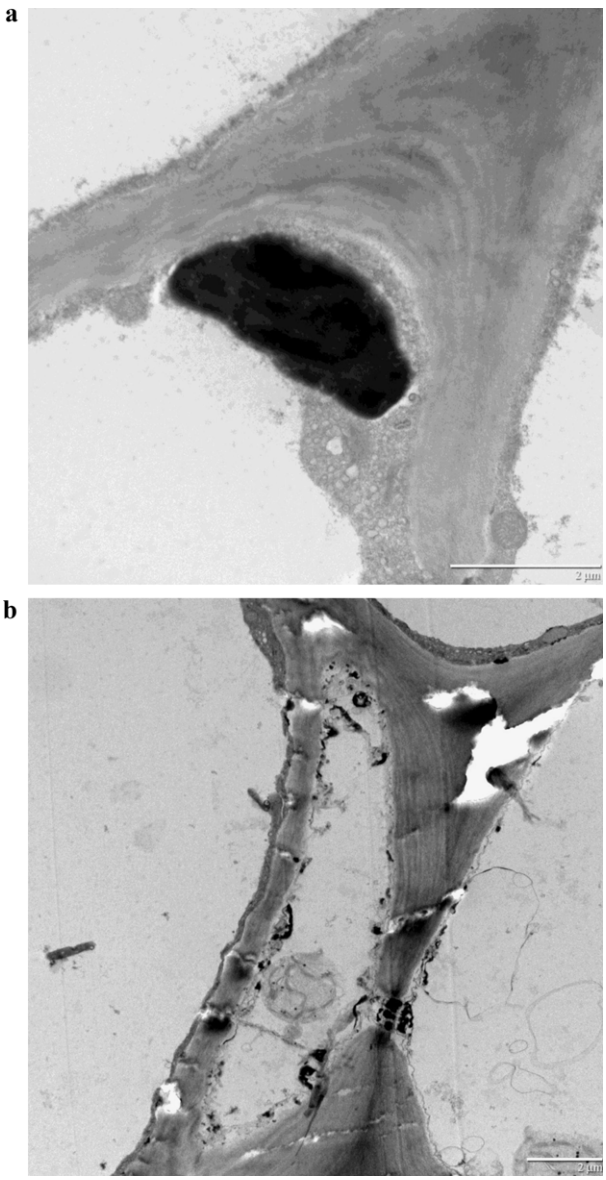

Fig. 7. (a) Transmission electron photomicrograph, longitudinal cross section of trichome cell tip with electron dense material, 80 kV, 33,000×. (b) Longitudinal cross section of trichome cell, 62Kx. Plasmodesmata to right of image with electron dense material.

showed that Indian mustard [*Brasscia juncea* L. (Salt et al., 1995)] and tobacco [*Nicotiana tabacum L.* (Choi et al., 2001)] concentrate Cd in trichomes. In the case of tobacco (Choi et al., 2001), secretory trichomes excreted Cd as crystals on the trichome tip, a mechanism we did not observe, nor did others cited (Salt et al., 1995; Isaure et al., 2006; Hu et al., 2012). Overall, it is likely that excess Zn and Cd are stored in trichomes in the same location and by similar mechanisms, but this remains to be demonstrated in realistic metal-enriched soils with plants grown more than 2 weeks.

The unique "spot bands" we observed reflect localized concentrations of Si and Zn in a trichome vacuole or cell wall. These patterns may have been previously unnoticed because the plant material was coated prior to X-ray analysis. The elevated Si levels may help aid Zn and Cd tolerance (Liang et al., 2007; Bauer et al., 2011). Silicon is thought to play a role in reducing Zn and Cd uptake and toxicity both as an agent to increase soil pH and as a direct detoxifier (Shi et al., 2005; Liang et al., 2005; Gu et al., 2011, 2012).

Fig. 8. TEM image, longitudinal cross section of epidermal cell adjacent to trichome, 41Kx. The black sharp-edged chain-like structures are SiO_2.

Increased Si concentrations have been observed in association with high Mn concentrations in trichomes on the leaves of pumpkin [(*Cucurbita moschata*) Duchesne ex Lam. Duchesne ex Poir.] (Iwasaki and Matsumura, 1999) and cucumber (*Cucumis sativus* L) (Horiguchi, 1987). In those plants Si was observed to alleviate Mn toxicity, thus allowing Mn to accumulate at the base of the trichomes without the development of necrotic lesions. Si-mediated Mn tolerance in leaf tissues other than trichomes has also been reported, with Si leading to increased Mn binding to cell walls (Iwasaki et al., 2002; Rogalla and Römheld, 2002; Liang et al., 2007; Bauer et al., 2011).

Neumann and zur Nieden (2001) and Neumann and De Figueiredo (2002) also found Zn co-localized with Si in *A. halleri*, *T. caerulescens* and three other European Zn hyperaccumulators in cell wall invaginations and vacuoles in epidermal and mesophyll cells. Wild plants were collected directly from a Zn mining area. The dark electron-dense areas which corresponded to high concentrations of Zn and Si were very similar to those we observed. These authors concluded that after uptake Zn is temporarily stored as zinc silicate, which degrades to SiO_2 and ionic Zn; the latter is then sequestered in vacuoles to ameliorate long-term toxicity. Trichomes on these plants were not investigated, probably because the study utilized numerous plants, all requiring ultrathin sections for transmission electron microscopy, and it is difficult to get a clean section of a trichome for any one plant just by chance.

While we could not identify Zn silicate in our samples, the strong correlation between Zn, Mn and traces of Cu and Ni with Si in the trichomes, and the presence of intercellular SiO_2 provides evidence for a generalized silicate stabilization mechanism for metal detoxification. New investigations into the relationship between Si and various hyperaccumulated metals are warranted. Note that this relationship is potentially masked by the typical hydroponic systems utilized for hyperaccumulator research since the levels of silica in deionized water are lower than what is available in soil. For example, Gu et al. (2012) found that Si decreased Zn toxicity in rice (*Oryza sativa* L.) simply by adding levels of silicic acid to a hydroponic culture system. At the highest level of Si addition, growth inhibition by 200 μM Zn was greatly reduced. However, the total amount of Zn in the seedlings did not differ among treatments, only the partitioning of Zn within the plant. Silicate addition increased the amount of Zn bound to cell wall, almost certainly a less toxic

location. As mentioned above, Si increased Mn binding to cell walls (Iwasaki et al., 2002; Rogalla and Römheld, 2002; Liang et al., 2007; Bauer et al., 2011) reducing Mn toxicity. It is plausible that Si plays a similar role in *P divaricata*, assisting in metal localization within the trichome, possibly in the form of Zn/Mn silicate.

The trichomes were also consistently enriched in Ca, with especially high concentrations of Ca and P in the distal bifurecated tips. A very similar high concentration of Ca and P was found at the distal tip of trichomes on the leaf surface of *Leontodon hispidus* L. (Asteraceae) when they were grown with 15 mM Ca in the rhizosphere (De Silva et al., 2001). It was inferred that some of the Ca at the tip was in a form of Ca phosphate. *L. hispidus* and *Centaurea scabiosa* L., which was also studied, are calcicoles, and their respective trichomes are believed to play a storage and regulatory role to prevent excess Ca from interfering with guard cells or entering the general epidermis. Excess Ca is stored mainly in the form of calcium oxalate in both species (De Silva et al., 1996). In *A. halleri*, Ca was elevated in the middle and tip portions of trichomes as compared to other leaf tissues (Küpper et al., 2000; Zhao et al., 2000). Phosphorus tended to be concentrated toward the tip of the trichome, but the localization was not mapped, so is not as specific as that we observed.

Although *Alyssum* is a serpentine plant, which is adapted to ultramafic soils relatively enriched in Mg as opposed to Ca, it nonetheless strongly concentrates Ca in the form of $CaCO_3$ (calcite form) nodules in the trichomes (Broadhurst et al., 2004, 2009; Tappero, 2008). Thus, in five distinct genera adapted to high environmental metal concentrations there is evidence for a Ca regulatory role for the trichome.

While *P. divaricata* has not been explicitly described as a calcicole, there is no reason why it could not be one, given the large extent of limestone and dolomite in the Lanping lead–zinc mining district (Kporfor and Jiagou, 2005; Chi et al., 2007). A relatively high Cd soil area where *P. divaricata* and *Picris hieraciodes* (see Yanqun et al., 2005) were collected is located in the Jinding/Lanping deposits, which consist of mineralized hydrothermal sand-veins injected into brecciated (heavily fractured and recemented) limestone and sometimes sandstone. Jinding/Lanping is sedimentary in origin and does not have massive sulfide bodies, but does have some large sulfide-bearing veins (Choi et al., 2001). Additionally the mineland soil utilized by Tang et al. (2009) was pH 7.44, indicative of a limestone or dolomite substrate, and in our experiments we were unable to sustain healthy growth in acidic soils.

In our experiment and that of Küpper et al. (2000) soil levels of Ca were normal, yet we still observed the distinct Ca and P pattern at the trichome tip that De Silva et al. (2001) reported. This suggests that the trichome tip is more than just a calcium phosphate "storehouse" for calcicoles but rather another aspect of a broad model of trichomes as important tissues for metal detoxification. Enough information exists now that we can view nonsecretory trichomes from many plant families as perhaps having a common origin as tissues adapted to handle a variety of environmental metals.

Acknowledgements

We thank Dr. Carrie L. Green, USDA Beltsville for ICP-MS analyses and Dr. Wen-An Chiou, University of Maryland NanoCenter for assistance in identifying SiO_2 in TEM sections.

References

Bauer, P., Elbaum, R., Weiss, I.M., 2011. Calcium and silicon mineralization in land plants: transport, structure and function. Plant Science 180, 746–756.

Broadhurst, C.L., Chaney, R.L., Angle, J.A., Maugel, T.K., Erbe, E.F., Murphy, C.A., 2004. Simultaneous hyperaccumulation of nickel, manganese and calcium in alyssum leaf trichomes. Environmental Science and Technology 38, 5797–5802.

Broadhurst, C.L., Tappero, R.V., Maugel, T.K., Erbe, E.F., Sparks, D.L., Chaney, R.L., 2009. Interaction of nickel and manganese in accumulation and localization in leaves of the Ni hyperaccumulators *Alyssum murale* and *Alyssum corsicum*. Plant Soil 314, 35–48.

Broadhurst, C.L., Sparks, D.A., Davis, A.P., Chaney, R.L. Relationship of nickel, manganese and sulfur and Ni-induced sulfur deficiency in the Ni-hyperaccumulator *Alyssum murale*. International Journal of Phytoremediation, submitted for publication.

Cai, S., Yue, L., Shang, Q., Nordberg, G., 1995. Cadmium exposure among residents in an area contaminated by irrigation water in China. WHO Bulletin 73, 359–367.

Cai, S., Yue, L., Shang, Q., Nordberg, G., 1998. Renal dysfunction from cadmium contamination or irrigation water: dose–response analysis in a Chinese population. WHO Bulletin 76, 153–159.

Cai, S., Yue, L., Hu, Z., Zhong, X., Ye, Z., Xu, H., Liu, Y., Rongdi Ji, R., Zhang, W., Zhang, F., 1990. Cadmium exposure and health effects among residents in an irrigation areas with ore dressing wastewater. Science of the Total Environment 90, 67–73.

Chaney, R.L., Reeves, P.G., Ryan, J.A., Simmons, R.W., Welch, R.M., Angle, J.S., 2004. An improved understanding of soil Cd risk to humans and low cost methods to phytoextract Cd from contaminated soils to prevent soil Cd risks. BioMetals 17, 549–553.

Chi, G., Xue, C., Lai, J., Qing, H., 2007. Sand injection and liquefaction structures in the Jinding Zn–Pb deposit Yunnan, China: indicators of an overpressured fluid system and implications for mineralization. Economic Geology 102, 739–743.

Choi, Y., Harada, E., Wada, H., Tsuboi, Y., Morita, T., Kusano, S.H., 2001. Detoxification of cadmium in tobacco plants: formation and active excretion of crystals containing cadmium and calcium through trichomes. Planta 21, 45–50.

De Silva, D.L.R., Hetherington, A.M., Mansfield, T.A., 1996. Where does all the calcium go? Evidence of an important regulatory role for trichomes in two calcicoles. Plant, Cell and Environment 19, 880–886.

De Silva, D.L., Mansfield, T.A., McAinsh, M.R., 2001. Changes in stomatal behaviour in the calcicole *Leontodon hispidus* due to the disruption by ozone of the regulation of apoplastic Ca^{2+} by trichomes. Planta 214, 158–162.

Faucon, M.-P., Shutcha, M.N., Meerts, P., 2007. Revisting copper and cobalt concentrations in supposed hyperaccumulators from SC Africa: influence of washing and metal concentrations in soil. Plant Soil 301, 29–36.

Frey, B., Keller, C., Zierold, K., Schulin, R., 2000. Distribution of Zn in functionally different leaf epidermal cells of the hyperaccumulator *Thlaspi caerulescens*. Plant, Cell and Environment 23, 675–687.

Gu, H.-H., Qiu, H., Tian, T., Zhan, S.-S., Deng, T.-H.-B., Chaney, R.L., Wang, S.-Z., Tang, Y.-T., Morel, J.-L., Qiu, R.-L., 2011. Mitigation effects of silicon rich amendments on heavy metal accumulation in rice (*Oryza sativa* L.) planted on multi-metal contaminated soil. Chemosphere 83, 1234–1240.

Gu, H.-H., Zhan, S.-S., Wang, S.-Z., Tang, Y.-T., Chaney, R.L., Fang, X.-H., Cai, X.-D., Qiu, R.-L., 2012. Silicon-mediated amelioration of zinc toxicity in rice (*Oryza sativa* L.) seedlings. Plant Soil 350, 193–204.

Horiguchi, T., 1987. Mechanism of manganese toxicity and tolerance of plants. II. Deposition of oxidized manganese in plant tissues. Soil Science and Plant Nutrition 33, 595–606.

Hu, P.J., Gan, Y.-Y., Tang, Y.-T., Zhang, Q.-F., Jiang, D., Yao, N., Rong-Liang Qiu, R.-L., 2012. Cellular tolerance, accumulation and distribution of cadmium in leaves of hyperaccumulator *Picris divaricata*. Pedosphere 22, 497–507.

Isaure, M.-P., Fayard, B., Sarret, G., Pairis, S., Bourguignon, J., 2006. Localization and chemical forms of cadmium in plant samples by combining analytical electron microscopy and X-ray spectromicroscopy. Spectrochimica Acta 61, 1242–1252.

Iwasaki, K., Matsumura, A., 1999. Effect of silicon on alleviation of manganese toxicity in pumpkin (*Curcubita moschata* Duch cv. Shintosa). Soil Science and Plant Nutrition 45, 909–920.

Iwasaki, K., Maier, P., Fecht, M., Horst, W.J., 2002. Leaf apoplastic silicon enhances manganese tolerance of cowpea (*Vigna unguiculata*). Journal of Plant Physiology 159, 167–173.

Kobayashi, J., 1978. Pollution by cadmium and the itai-itai disease in Japan. In: Oehme, F.W. (Ed.), Toxicity of Metals in the Environment. Marcel Dekker, New York, pp. 199–260.

Kporfor, J., Jiagou, C., 2005. Prediction of hydrothermal copper, gold, silver and lead–zinc in northwestern Yunnan using weight of evidence model. Geospatial Information Science 8, 230–234.

Küpper, H., Lombi, E., Zhao, F.-J., McGrath, S.P., 2000. Cellular compartmentation of cadmium and zinc in relation to other metals in the hyperaccumulator *Arabidopsis halleri*. Planta 212, 75–84.

Küpper, H., Zhao F.-J., McGrath, S.P., 1999. Cellular compartmentation of zinc in the leaves of the hyperaccumulator *Thlaspi caerulescens*. Plant Physiology 119, 305–311.

Leitenmaier, B., Küpper, H., 2011. Cadmium uptake and sequestration kinetics in individual leaf cell protoplasts of the Cd/Zn hyperaccumulator *Thlaspi caerulescens*. Plant, Cell and Environment 34, 208–219.

Li, J.T., Liao, B., Lan, C.Y., Ye, Z.H., Baker, A.J.M., Shu, W.S., 2010. Cadmium tolerance and accumulation in cultivars of a high-biomass tropical tree (*Averrhoa carambola*) and its potential for phytoextraction. Journal of Environment Quality 39, 1262–1268.

Liang, Y., Wong, J.W.C., Wei, L., 2005. Silicon-mediated enhancement of cadmium tolerance in maize (*Zea mays* L.) grown in cadmium contaminated soil. Chemosphere 58, 475–483.

Liang, Y., Sun, W., Zhu, Y.-G., Christie, P., 2007. Mechanisms of silicon-mediated alleviation of abiotic stresses in higher plants: a review. Environmental Pollution 147, 422–428.

Neumann., D., De Figueiredo, C., 2002. A novel mechanism of silicon uptake. Protoplasma 220, 59–67.
Neumann, D., zur Nieden, U., 2001. Silicon and heavy metal tolerance of higher plants. Phytochemistry 56, 685–692.
Phaenark, C., Pokethitiyook, P., Kruatrachue, M., Ngernsansarua, C., 2009. Cd and Zn accumulation in plants from the Padaeng zinc mine area. International Journal of Phytoremediation 11, 479–495.
Rogalla, H., Römheld, V., 2002. Role of leaf apoplast in silicon-mediated manganese tolerance of *Cucumis sativus* L. Plant, Cell and Environment 25, 549–555.
Salt, D.E., Prince, R.C., Pickering, I.C., Raskin, I., 1995. Mechanisms of cadmium mobility and accumulation in Indian mustard. Plant Physiology 109, 1427–1433.
Shi, X.H., Zhang, C.C., Wang, H., Zhang, F.S., 2005. Effect of Si on the distribution of Cd in rice seedlings. Plant Soil 272, 53–60.
Tang, Y.-T., Qiu, R.-L., Zeng, X., Fang, X., Yu, F., Zhou, X., Wu, Y., 2009. Zn and Cd hyperaccumulating characteristics of *Picris divaricata* Vant. International Journal of Environment Pollution 38, 26–38.
Tappero, R.V., 2008. Microspectroscopic study of cobalt speciation and localization in nickel hyperaccumulator *Alyssum murale*. Ph.D. Dissertation. University of Delaware, Newark, DE.
Teeyakasem, W., Nishijo, M., Honda, R., Satarug, S., Swaddiwudhipong, W., Ruangyuttikarn, W., 2007. Monitoring of cadmium toxicity in a Thai population with high-level environmental exposure. Toxicology Letters 169, 185–195.
van der Ent, A., Baker, A.J.M., Reeves, R.D., Pollard, A.J., Schat, H., 2012. Hyperaccumulators of metal and metalloid trace elements: facts and fiction. Plant Soil, http://dx.doi.org/10.1007/s11104-012-1287-3.
Yanqun, Z., Yuan, L., Jianjun, C., Haiyan, C., Li, Q., Schvartz, C., 2005. Hyperaccumulation of Pb, Zn and Cd in herbaceous *(sic)* grown on lead–zinc mining area in Yunnan, China. Environment International 31, 755–762.
Ying, R.-R., Qiu, R.-L., Tang, Y.-T., Hu, P.-J., Qiu, H., Chen, H.-R., Shi, T.-H., Morel, J.-L., 2010. Cadmium tolerance of carbon assimilation enzymes and chloroplast in Zn/Cd hyperaccumulator *Picris divaricata*. Journal of Plant Physiology 167, 81–87.
Zhao, F.-J., Lombi, E., Breedon, T., McGrath, S.P., 2000. Zinc hyperaccumulation and cellular distribution in *Arabidopsis halleri*. Plant, Cell and Environment 23, 507–514.